Development 127, 2573-2582 (2000)
Printed in Great Britain © The Company of Biologists Limited 2000
DEV4360

The bHLH transcription factor Hand2 plays parallel roles in zebrafish heart and pectoral fin development

Deborah Yelon[1,*,‡], Baruch Ticho[2], Marnie E. Halpern[3], Ilya Ruvinsky[4], Robert K. Ho[4], Lee M. Silver[4] and Didier Y. R. Stainier[1,‡]

[1]Department of Biochemistry and Biophysics and Programs in Developmental Biology, Genetics and Human Genetics, University of California, San Francisco, San Francisco, CA, USA
[2]Department of Pediatrics, Harvard Medical School, Boston, MA, USA
[3]Department of Embryology, Carnegie Institution, Baltimore, MD, USA
[4]Department of Molecular Biology, Princeton University, Princeton, NJ, USA
*Present address: Developmental Genetics Program, Skirball Institute, NYU School of Medicine, New York, NY, USA
‡Authors for correspondence (e-mail: didier_stainier@biochem.ucsf.edu; e-mail: yelon@saturn.med.nyu.edu)

Accepted 29 March; published on WWW 23 May 2000

SUMMARY

The precursors of several organs reside within the lateral plate mesoderm of vertebrate embryos. Here, we demonstrate that the zebrafish *hands off* locus is essential for the development of two structures derived from the lateral plate mesoderm – the heart and the pectoral fin. *hands off* mutant embryos have defects in myocardial development from an early stage: they produce a reduced number of myocardial precursors, and the myocardial tissue that does form is improperly patterned and fails to maintain *tbx5* expression. A similar array of defects is observed in the differentiation of the pectoral fin mesenchyme: small fin buds form in a delayed fashion, anteroposterior patterning of the fin mesenchyme is absent and *tbx5* expression is poorly maintained. Defects in these mesodermal structures are preceded by the aberrant morphogenesis of both the cardiogenic and forelimb-forming regions of the lateral plate mesoderm. Molecular analysis of two *hands off* alleles indicates that the *hands off* locus encodes the bHLH transcription factor Hand2, which is expressed in the lateral plate mesoderm starting at the completion of gastrulation. Thus, these studies reveal early functions for Hand2 in several cellular processes and highlight a genetic parallel between heart and forelimb development.

Key words: Lateral plate mesoderm, Forelimb, *hands off*, *tbx5*, *sonic hedgehog*, Zebrafish

INTRODUCTION

In vertebrate embryos, derivatives of the lateral plate mesoderm (LPM) include a number of discrete tissue types such as the heart, endothelium, blood, connective tissue, smooth muscle and chondrogenic portion of the limbs. The genetic regulation of LPM patterning and differentiation is undoubtedly complex, and the precise steps that convert undifferentiated LPM into these distinct organs remain unknown.

The patterning of the cardiogenic region of the LPM is especially intricate. In zebrafish, for example, a number of genes (e.g. *gata4*, *gata5*, *gata6*, *hand2* and *tbx5*) are expressed bilaterally in a large portion of the LPM from the completion of gastrulation (Serbedzija et al., 1998; Reiter et al., 1999; Ruvinsky et al., 2000; Begemann and Ingham, 2000). During early somitogenesis stages, a specific anterior section of the LPM also expresses the NK-class transcription factor gene *nkx2.5*, considered an early marker of precardiac mesoderm (Chen and Fishman, 1996; Lee et al., 1996). By mid-somitogenesis, an anterior subset of these *nkx2.5*-expressing cells go on to express myocardial-specific genes (Yelon et al., 1999) and contribute to the myocardium (Serbedzija et al., 1998). These myocardial precursors are further subdivided prior to cardiac fusion into preventricular and preatrial cells, as evidenced by the restricted expression of chamber-specific markers (Yelon et al., 1999). Thus, a detailed pattern of gene expression is established within the anterior LPM well before heart tube formation.

Only a few regulators of pattern formation within the cardiogenic LPM have been identified. The secreted growth factors Bmp2 and Fgf8 and the transcription factor Gata5 contribute to the regulation of *nkx2.5* expression (Kishimoto et al., 1997; Schultheiss et al., 1997; Reifers et al., 2000; Reiter et al., 1999). Signals from the embryonic midline may influence the induction of the myocardial precursors from among the *nkx2.5*-expressing precardiac cells (Goldstein and Fishman, 1998; Serbedzija et al., 1998). Finally, the subdivision of the myocardial precursors into preventricular and preatrial populations is likely to be influenced by the localization of retinoic acid (Chazaud et al., 1999; Niederreither et al., 1999; Xavier-Neto et al., 1999; Yelon and Stainier, 1999) as well as the transcription factor Irx4 (Bao et al., 1999; Bruneau et al., 2000).

In an effort to understand the genetic regulation of pattern formation within the LPM in greater detail, we have identified a number of zebrafish mutations that disrupt myocardial patterning (Alexander et al., 1998). Here, we demonstrate that the zebrafish *hands off* (*han*) locus plays an important role in the differentiation, patterning and morphogenesis of two distinct LPM derivatives – the myocardium and the pectoral fin mesenchyme. *nkx2.5*-expressing precardiac mesoderm forms in *han* mutants, but these cells cannot differentiate into properly patterned myocardial tissue. Similarly, the pectoral fin buds in *han* mutants arise but do not differentiate normally and fail to exhibit proper anteroposterior (AP) patterning.

Molecular analysis of two *han* alleles indicates that the *han* locus encodes the bHLH transcription factor Hand2, also known as dHAND/Thing-2/Hed (Cross et al., 1995; Hollenberg et al., 1995; Srivastava et al., 1995). *hand2* is expressed in the LPM of zebrafish, chick, frog, and mouse embryos (Cross et al., 1995; Hollenberg et al., 1995; Srivastava et al., 1995; Angelo et al., 2000). While targeted gene inactivation in the mouse previously implicated Hand2 in the later differentiation of the right ventricle (Srivastava et al., 1997), its broader role in the early stages of myocardial development as well as its role in forelimb development were not recognized. Thus, our studies reveal several essential early functions of Hand2. Moreover, the phenotypic analysis of *han* mutants highlights an intriguing genetic parallel between heart and forelimb development.

MATERIALS AND METHODS

Zebrafish

Adult fish and embryos were maintained and staged as previously described (Westerfield, 1995). Mutations were maintained by outcrossing heterozygous adults to standard wild-type strains; homozygous or *trans*heterozygous mutant embryos were generated by intercrossing heterozygotes. Some lines carried the *golden* mutation, which inhibits melanophore pigmentation and thereby facilitates inspection of internal organs (Streisinger et al., 1986).

The han^{s6} mutation was identified in a screen for ENU-induced mutations affecting MF20 and S46 immunostaining in haploid embryos (Alexander et al., 1998). We used a postmeiotic mutagenesis protocol that can induce an array of genetic lesions, including point mutations, deletions and translocations (Imai et al., 2000). The han^{c99} mutation was identified in an independent screen for gamma ray-induced mutations as part of the Zebrafish Deletion Project. Both mutations behave in a Mendelian recessive fashion with complete penetrance and embryonic lethality. han^{s6} and han^{c99} fail to complement each other: 157/601 embryos from *c99*/+ × *s6*/+ matings display the mutant phenotype.

Immunofluorescence and in situ hybridization

Whole-mount immunofluorescence, in situ hybridization and sectioning were performed as previously described (Yelon et al., 1999). The monoclonal antibodies MF20 (Bader et al., 1982) and S46 (generous gift of Dr Frank Stockdale) were used. MF20 was obtained from the Developmental Studies Hybridoma Bank, maintained by the Department of Biological Sciences, University of Iowa, under contract NO1-HD-2-3144 from the NICHD.

Genomic DNA and cDNA analysis

Genomic DNA extraction was performed as previously described (Reiter et al., 1999) or with a Nucleon kit (Scotlab). PCR strategies were standard, except for the use of eLONGase enzyme mix (BRL) for long-range amplification. For cDNA analysis, total RNA was isolated using Trizol (BRL) and reverse transcribed using Superscript II (BRL). 5′ RACE (SMART RACE, Clontech) was performed in order to confirm the 5′ end of the *hand2* mRNA and to investigate the splice variants in han^{c99} mutants. All sequencing was performed using an ABI 377 system.

P1 artificial chromosome analysis

A zebrafish P1 artificial chromosome (PAC) library (Amemiya and Zon, 1999) was screened by PCR on pools of clones and by hybridization to high-density filters (RZPD, Berlin). Further analysis of *hand2*-containing PACs was conducted in an effort to estimate the size of the han^{s6} deletion. For example, we sequenced the ends of the *hand2*-containing PAC 57N7 and determined by PCR that both ends are present in han^{s6} genomic DNA. Since 57N7 contains a ~100 kb insert (determined by PFGE), we conclude that the han^{s6} deletion removes less than 100 kb of genomic DNA.

Mapping, linkage testing and genotyping

We placed han^{s6} on zebrafish linkage group 1 using half-tetrad analysis (Johnson et al., 1995) and mapped *hand2* to the same region (between z9409 and z21548) using the Goodfellow zebrafish radiation hybrid panel (Geisler et al., 1999; see http://wwwmap.tuebingen.mpg.de/). han^{s6} linkage testing was performed using a combination of four PCR primers that simultaneously amplify a *hand2* fragment and a fragment of the end of PAC 57N7 from individual diploid or haploid embryos. Oligonucleotides used were 5′-AATATTGAACTTGCAAACATA-CAAGC-3′, 5′-GTCTATATGAATTACACTCTAGTGG-3′, 5′-AATT-TCCCACTACGGACATTGGA-3′, and 5′-AGAGACAGAAATAGA-TAATGAACGT-3′. han^{c99} linkage testing was performed using a combination of three PCR primers that simultaneously amplify a fragment of *hand2* that spans the han^{c99} insertion and a fragment of the insertion from individual diploid or haploid embryos. The locations of these primers are indicated in Fig. 5C and typical results are shown in Fig. 5D. Oligonucletides used were 5′-TGATCACCCG-TTAATGTTCTTG-3′, 5′-CCCATGAAAAAGGTAAGAGTGAA-3′, and 5′-CGATTCAGACACCAACTGTCTC-3′. The same oligonucleotide mixes were used to genotype han^{s6} or han^{c99} embryos following in situ hybridization.

Microinjection

Capped synthetic *hand2* and *lacZ* mRNA were generated using pCS2:*hand2*, SP64TK:*lacZ* and the mMessage mMachine system (Ambion). Embryos were injected with 100-500 pg of *hand2* or *lacZ* mRNA at the 1- to 4-cell stage.

RESULTS

The zebrafish *hands off* locus

In the course of a screen for zebrafish mutations affecting myocardial development (Alexander et al., 1998), we identified *s6*, an ENU-induced mutation that causes severe heart, jaw and pectoral fin defects. We named the locus represented by this mutation *hands off* (*han*), primarily because of its lack of pectoral fins, which are the teleost equivalents of tetrapod forelimbs (Grandel and Schulte-Merker, 1998). A gamma ray-induced non-complementing allele (see Materials and Methods), han^{c99}, causes a very similar array of defects that are generally less severe. Here, we use these two mutant alleles to investigate the role of *han* in heart and forelimb development; the role of *han* in jaw development will be discussed elsewhere (C. Miller, D. Y., D. Y. R. S. and C. Kimmel, unpublished data).

han is essential for myocardial differentiation, patterning and morphogenesis

Cardiovascular defects are morphologically apparent in *han*^{s6} mutant embryos by 24 hours postfertilization (hpf). It is difficult to detect any contracting tissue or circulating blood and a mild pericardial edema is present (Fig. 1A,B). Immunodetection of cardiac myosin heavy chain molecules (Fig. 1C,D) and examination of *cardiac myosin light chain 2* (*cmlc2*) (Fig. 1E,F) expression revealed that extremely little myocardial tissue forms in *han*^{s6} mutants. Furthermore, while wild-type embryos form a single midline heart tube, *han*^{s6} mutants develop two small lateral clusters of myocardial cells that never fuse together at the midline (Fig. 1C-F). The wild-type heart is clearly divided into two distinct chambers – an anterior ventricle and a posterior atrium – but the *han*^{s6} myocardial tissue is primarily atrial, as indicated by S46 immunostaining (Fig. 1C,D). Correspondingly, the expression of *ventricular myosin heavy chain* (*vmhc*) is strongly affected; some *han*^{s6} mutants do not express *vmhc* at all, while others show an irregular distribution of *vmhc* in a few myocardial cells (Fig. 1G,H).

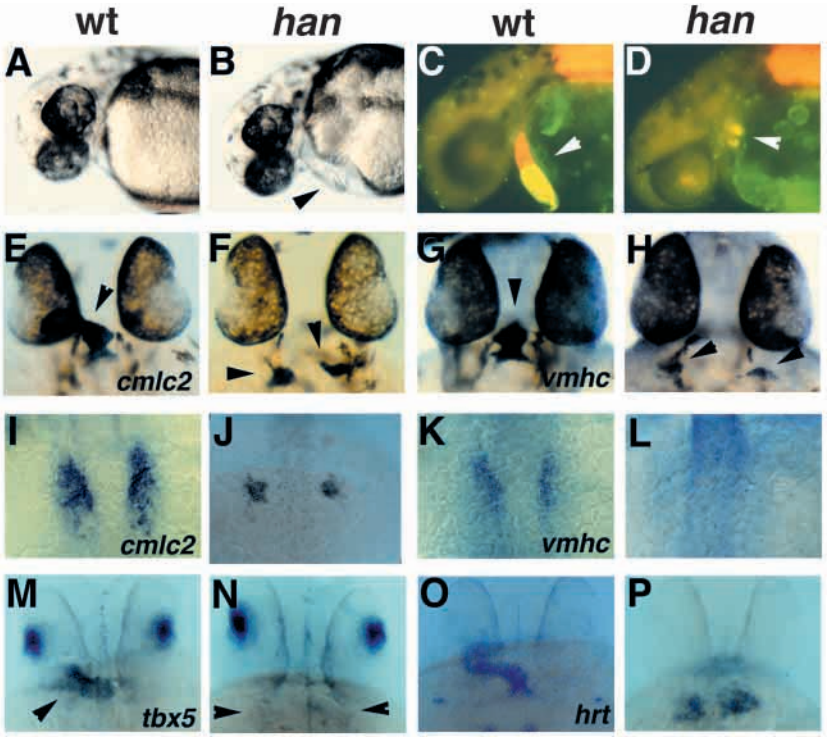

Fig. 1. Myocardial defects in *han*^{s6} mutants. (A,C,E,G,I,K,M,O) Wild-type embryos; (B,D,F,H,J,L,N,P) *han*^{s6} mutant siblings. (A-D) Lateral views at 36 hpf, anterior to the left. (A,B) Bright-field images; mutants (B) display mild pericardial edema (arrowhead). (C,D) Immunofluorescent images of embryos stained with MF20 (TRITC) and S46 (FITC). In these double exposures, red fluorescence indicates MF20 staining of ventricular and somitic tissue, while yellow fluorescence indicates the overlap of S46 and MF20 staining in atrial tissue (Stainier and Fishman, 1992). (C) Wild-type embryos have a midline heart tube (arrowhead) with two distinct chambers, an anterior ventricle (red) and a posterior atrium (yellow). (D) *han*^{s6} mutants have two small clusters of myocardial tissue (arrowhead) that appear to be primarily atrial (yellow). (E-H, M-P) Dorsal views through the head at 33 hpf, anterior to the top. (M-P) are *golden* homozygotes. (I-L) Dorsal views of the myocardial precursors at the 15-somite stage (16.5 hpf). (E,F,I,J) In situ hybridization showing expression of the myocardial marker *cmlc2* (Yelon et al., 1999). (E) Wild-type embryos express *cmlc2* throughout the heart tube (arrowhead); (F) *han*^{s6} mutants have two small patches of *cmlc2*-expressing myocardial tissue (arrowheads). Younger wild-type embryos (I) have more myocardial precursors than *han*^{s6} mutant siblings (J). (G,H,K,L) Expression of the ventricular marker *vmhc* (Yelon et al., 1999). Wild-type embryos (G) express *vmhc* only within the future ventricle (arrowhead). *han*^{s6} mutants vary in amount of *vmhc*-expressing tissue: some *han*^{s6} mutants have no *vmhc* expression at this stage (data not shown), while others (H) have small populations of cells with weak *vmhc* expression (arrowheads). (K) Younger wild-type embryos express *vmhc* in a medial subset of myocardial precursors (Yelon et al., 1999); (L) *vmhc* expression is difficult to detect in *han*^{s6} mutants at this stage. (M,N) Expression of *tbx5* in dorsal retina and heart tube (arrowhead) is apparent in wild-type embryos (M), but only dorsal retina expression is detectable in *han*^{s6} mutants (N, arrowheads indicate location of myocardium). (O,P) Expression of *hrt* in myocardium is apparent in wild-type embryos (O) and in *han*^{s6} mutants (P).

These defects in the production and patterning of myocardial tissue are evident from an early stage in *han*^{s6} mutants. Even at the onset of myocardial differentiation at the 15-somite stage (16.5 hpf), *han*^{s6} mutants have noticeably fewer *cmlc2*-expressing myocardial cells than their wild-type siblings (Fig. 1I,J). As in older *han*^{s6} mutant embryos, small myocardial populations are clustered bilaterally and these cells rarely express *vmhc* (Fig. 1I-L).

Many myocardial genes are expressed robustly within the small populations of *han*^{s6} myocardial cells, including *bmp4*, *mef2c*, *gata4*, *gata5*, *gata6* and all of the cardiac contractile genes examined except *vmhc* (data not shown). The T-box transcription factor gene *tbx5* (Tamura et al., 1999; Ruvinsky et al., 2000; Begemann and Ingham, 2000) is a notable exception. Expression of *tbx5* in the LPM is initiated normally in *han*^{s6} mutants during early somitogenesis (data not shown), but the mutant myocardial cells fail to maintain *tbx5* expression. By 24 hpf, *tbx5* expression is significantly reduced in *han*^{s6} myocardial cells (Fig. 1M,N), while another myocardial T-box gene, *hrt* (Griffin et al., 2000), continues to be expressed at normal levels (Fig. 1O,P).

Thus, specific aspects of myocardial differentiation (production of *cmlc2*-expressing cells and maintenance of *tbx5* expression), patterning (*vmhc* expression) and morphogenesis (heart tube formation) are defective in *han*^{s6} mutants.

Normal precardiac mesoderm in *han* mutants

Although myocardial development is severely disrupted in *han*^{s6} mutants, the initial establishment of the precardiac mesoderm appears to proceed normally. *nkx2.5* is normally expressed in bilateral populations of precardiac cells from early somitogenesis stages (Chen and Fishman, 1996; Lee et al., 1996); *han*^{s6} mutants and wild-type siblings are indistinguishable in this regard (Fig. 2A,B). In wild-type embryos, most, but not all, of these *nkx2.5*-expressing cells go on to express myocardial genes like *cmlc2* (Yelon et al., 1999) and contribute to the myocardium (Serbedzija et al., 1998). However,

in *han*^{s6} mutants, very few *nkx2.5*-expressing cells go on to express *cmlc2* or other myocardial genes (Fig. 1I,J). Therefore, the failure of *han*^{s6} mutants to produce normal numbers of myocardial cells is not due to a deficiency of precardiac mesoderm. The initiation of myocardial differentiation in a subset of *nkx2.5*-expressing cells represents a specific developmental transition that does not proceed efficiently in *han*^{s6} mutants.

Early expansion of the cardiogenic LPM depends on *han* function

During the initiation of myocardial differentiation in zebrafish, the anterior LPM undergoes an apparent expansion. At the completion of gastrulation, LPM markers like *gata4* are expressed in narrow bilateral stripes of cells (Fig. 2C); wild-type and *han*^{s6} mutant embryos appear identical in their expression of LPM markers from the tailbud stage until the 10-somite stage (data not shown). Between the 10-somite (14 hpf) and 15-somite (16.5 hpf) stages in wild-type embryos, these gene expression patterns change; the domains of LPM marker expression gradually expand mediolaterally. By the 15-somite stage, LPM genes are expressed in significantly broader bilateral sheets of cells in wild-type embryos (Fig. 2D). This transition from narrow to broader domains of LPM gene expression is profoundly affected in *han*^{s6} mutants. For example, at the 15-somite stage, *han*^{s6} mutants still exhibit narrow bilateral stripes of *gata4* expression; no expansion has occurred (Fig. 2E). By 24 hpf, this tissue appears narrow and dysmorphic (Fig. 2G) in comparison to the continuous sheet of *gata4*-expressing cells found in wild-type siblings (Fig. 2F).

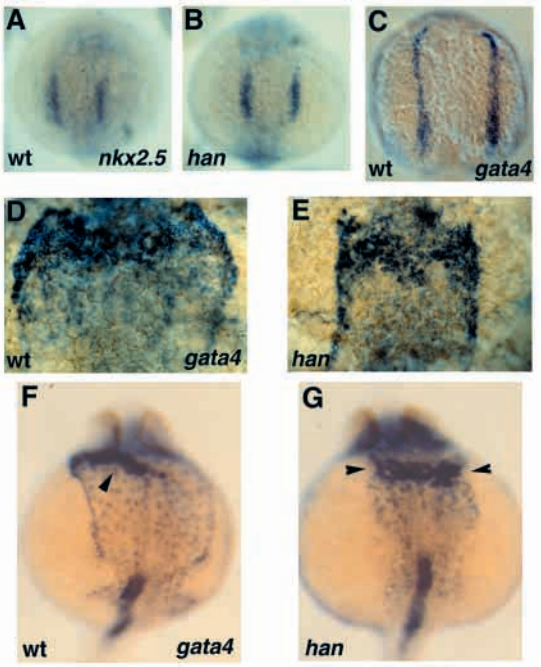

Fig. 2. Normal precardiac mesoderm and aberrant LPM development in *han*^{s6} mutants. (A,B) Dorsal views at the 10-somite stage (14 hpf), anterior to the top. Wild-type (A) and *han*^{s6} mutant (B) siblings have indistinguishable *nkx2.5* expression. (C-G) Dorsal views, anterior to the top, of *gata4* expression at the 5-somite stage (approximately 12 hpf) (C), 15-somite stage (D,E) and 24 hpf (F,G). (C) Expression of *gata4* in the anterior LPM begins in narrow bilateral stripes of cells that fuse medially by the 20-somite stage. (D) Before cardiac fusion begins, the *gata4* expression domain has become much wider mediolaterally in wild-type embryos. (E) However, in *han*^{s6} mutants, *gata4* expression remains as narrow bilateral stripes. (G) *gata4* expression is maintained in the LPM and myocardia (arrowheads) of *han*^{s6} mutants. (F) The mutant LPM is narrow and dysmorphic in comparison to the broad sheet of *gata4*-expressing LPM in wild-type siblings (arrowhead indicates heart tube). We have obtained similar results with all other LPM markers, including *gata5*, *gata6* and *tbx5*; that is, the expression domains of these genes expand in wild-type embryos but not in *han*^{s6} mutants.

han is essential for pectoral fin differentiation, patterning and morphogenesis

Having identified significant defects in the cardiogenic portion of the *han*^{s6} LPM, we proceeded to examine the formation of other LPM derivatives in *han*^{s6} mutants and found profound defects in pectoral fin development. In wild-type embryos, pectoral fin mesenchyme proliferates to form bilateral fin buds (Grandel and Schulte-Merker, 1998), but this process is significantly delayed in *han* mutants (Fig. 3A,B). The wild-type fin gradually elongates and comes to be composed of a central chondrogenic condensation flanked by myogenic mesenchyme (Grandel and Schulte-Merker, 1998); in contrast, *han*^{s6} mutants have a small bud of undifferentiated mesenchyme that fails to elongate or form a chondrogenic condensation (Fig. 3C,D). The mutant pectoral fin mesenchyme expresses *tbx5*, although, in comparison to wild type, expression is not well maintained after 24 hpf (Fig. 3A-D and data not shown). The pectoral fin defects are unlikely to be secondary consequences of the lack of circulation, since many zebrafish mutants with severe cardiac defects exhibit normal pectoral fin development (Chen et al., 1996; Stainier et al., 1996).

In zebrafish and other vertebrates, limb outgrowth is dependent upon proper limb bud patterning (Johnson and Tabin, 1997; Martin, 1998). The expression of *sonic hedgehog* (*shh*) in a posterior region of the pectoral fin bud (the zone of polarizing activity, or ZPA) is an important influence on fin AP patterning (Neumann et al., 1999; Schauerte et al., 1998). *han*^{s6} mutants never express *shh* in their pectoral fin buds at any stage, but *shh* expression in *han*^{s6} endoderm and ventral neuroectoderm is normal (Fig. 3E). It is not known precisely how the posterior restriction of *shh* expression is regulated, although some early indications of limb AP patterning have been shown to be *shh*-independent in the zebrafish (Neumann et al., 1999). For example, initiation of *hoxd-11*, *hoxd-12* and *bmp2* expression in a posterior portion of the pectoral fin mesenchyme occurs normally in zebrafish *sonic you* (*syu*) mutants that lack *shh* activity (Neumann et al., 1999). In contrast, *han* mutants do not display any features of AP patterning within the pectoral fin mesenchyme (Fig. 3F-I and data not shown).

We also examined the pectoral fin-forming region of the LPM at stages prior to fin bud formation. In wild-type embryos, LPM markers such as *tbx5* are first expressed in narrow stripes of the fin-forming region of the LPM (Ruvinsky et al., 2000; Begemann and Ingham, 2000). During segmentation stages, these expression domains expand mediolaterally (Fig. 3J,K), in a manner similar to the expansion of gene expression within the cardiogenic LPM.

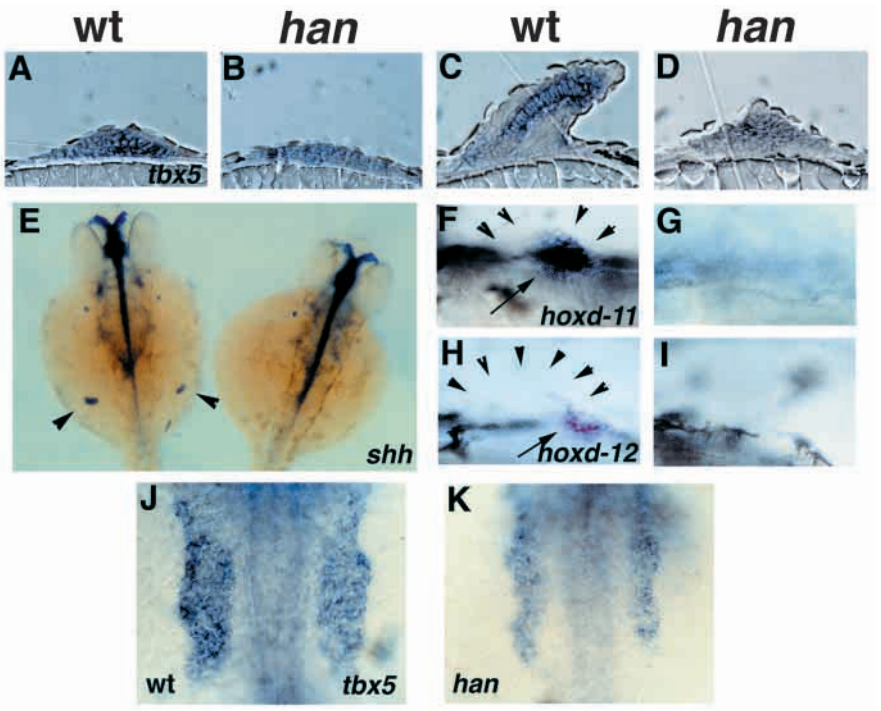

Fig. 3. Pectoral fin defects in *han*^{s6} mutants. (A-D) Longitudinal sections through pectoral fin buds after in situ hybridization for *tbx5* expression, anterior to the left. (A) At 32 hpf, a fin bud is forming in wild-type embryos. (B) *han*^{s6} mutants exhibit a delay in fin bud formation as well as a reduction in *tbx5* expression at this stage. (C) In 48 hpf wild-type embryos, the pectoral fin is elongating and a chondrogenic condensation is forming. *tbx5* expression is highest in the chondrogenic portion of the pectoral fin at this stage. (D) In *han*^{s6} mutants, a small undifferentiated fin bud expresses a reduced level of *tbx5*. (E) Dorsal views, anterior to the top, of a wild-type embryo (left) and a *han*^{s6} mutant (right) at 36 hpf. Embryos are *golden* homozygotes. *shh* expression is visible in the ZPA of each pectoral fin bud in wild-type embryos (arrowheads) but not in *han*^{s6} mutants. (F-I) Lateral views, anterior to the left, of pectoral fin buds from wild-type (F,H) and *han*^{s6} mutant (G,I) siblings at 32 hpf. (F) Wild-type embryos express *hoxd-11* in a posterior portion (arrow) of the fin bud (outline indicated by arrowheads); (G) *han*^{s6} mutants never express *hoxd-11* in the fin mesenchyme. (H) Wild-type embryos express *hoxd-12* in a posterior portion (arrow) of the fin bud (outline indicated by arrowheads); (I) *han*^{s6} mutants never express *hoxd-12* in the fin mesenchyme. (J,K) Dorsal views, anterior to the top, of the pectoral fin-forming region of the LPM in wild-type (J) and *han*^{s6} mutant (K) embryos at the 16-somite stage (17 hpf). The domain of *tbx5* expression is expanded in wild-type embryos, but not in *han*^{s6} mutants.

This process of expansion does not occur efficiently in *han*^{s6} mutants (Fig. 3J,K).

han^{c99} mutants have mild heart and fin defects relative to *han*^{s6} mutants

Examination of the less severely affected *han*^{c99} mutants confirmed the roles of *han* indicated by the *han*^{s6} phenotype. For example, the role of *han* in the generation of myocardial tissue is evident in *han*^{c99} homozygotes and *han*$^{s6/c99}$ *trans*heterozygotes (Fig. 4A-D). The lack of myocardial cells is most extreme in *han*^{s6} mutants (Fig. 4D) and most mild in *han*^{c99} mutants (Fig. 4B), with *trans*heterozygotes affected to an intermediate degree (Fig. 4C). Similarly, the failure to maintain myocardial *tbx5* expression is more severe in *han*^{s6} mutants (Fig. 4H) than in *han*^{c99} mutants (Fig. 4F) or *trans*heterozygotes (Fig. 4G), confirming that *han* regulates *tbx5* maintenance. Furthermore, comparisons of *vmhc* expression indicated reduced amounts of ventricular tissue in *han*^{c99} mutants and in *trans*heterozygotes (data not shown), reinforcing the conclusion that *han* is essential for ventricular differentiation.

Phenotypic comparisons also indicated the role of *han* in the regulation of cardiac fusion (Fig. 4A-H). While the bilateral myocardial populations in *han*^{s6} mutants never fuse (Fig. 4D and data not shown), the myocardial cells in *han*^{c99} mutants (Fig. 4B,F) and *trans*heterozygotes (Fig. 4C,G) fuse slowly in comparison to wild-type embryos and form small heart tubes (data not shown).

Examination of younger embryos demonstrated that *han* function regulates the extent of expansion of *gata4* expression in the LPM (Fig. 4I-L). Slightly expanded domains of *gata4* expression do form in *han*^{c99} mutants (Fig. 4J) and *trans*heterozygotes (Fig. 4K) show signs of irregular LPM morphogenesis. Furthermore, analysis of *cmlc2* expression at this stage verified that *han* controls the early production of myocardial precursors (Fig. 4M-O). The number of *cmlc2*-expressing cells is clearly reduced in *han*^{c99} mutants relative to wild type (Fig. 4M,N), although not as dramatically as in *han*^{s6} mutants (Fig. 4O).

In contrast to their distinct cardiac phenotypes, the *han*^{s6} and *han*^{c99} pectoral fin phenotypes are quite similar. Neither the *han*^{c99} nor the *han*^{s6} pectoral fins elongate, maintain *tbx5* expression effectively, express *shh*, *hoxd-11* and *hoxd-12*, or exhibit normal expansion of *tbx5* expression in the fin-forming LPM (data not shown). Maintenance of gene expression in the apical epidermal fold of the pectoral fin is regulated by *shh* in the zebrafish (Neumann et al., 1999), so neither *han*^{s6} nor *han*^{c99} mutants maintain apical fold gene expression well (Fig. 4P-R). Even so, *han*^{c99} mutants have detectable *dlx2* expression in the apical fold more often than *han*^{s6} mutants do (8 of 8 *han*^{c99} cases and only 5 of 10 *han*^{s6} cases). This distinction suggests that some level of mesenchyme differentiation and/or patterning may be initiated, but not maintained, in *han*^{c99} fin buds.

Altogether, the relationships between the *han*^{s6}, *han*^{c99} and *trans*heterozygote phenotypes lead to the hypothesis that *han*^{s6} represents a null allele, while *han*^{c99} retains partial *han* function.

The *han* locus encodes the bHLH transcription factor Hand2

In search of the genetic defect responsible for the *han* mutant phenotypes, we considered candidate genes known to be expressed in the heart, forelimb and jaw. The bHLH transcription factor gene *hand2* is expressed in these tissues in

mouse and chick embryos (Cross et al., 1995; Hollenberg et al., 1995; Srivastava et al., 1995). Moreover, we mapped the *han*^{s6} mutation and a zebrafish *hand2* homolog (Angelo et al., 2000) to the same region of zebrafish linkage group 1 (see Materials and Methods). We therefore proceeded to test whether *han* encoded zebrafish Hand2.

The genomic structure of zebrafish *hand2* is relatively simple: the entire transcribed region (1.6 kb) is contained within two exons separated by a ~200 bp intron (Fig. 5A). Extensive PCR and Southern blot analyses indicate that the entire *hand2* locus is deleted from *han*^{s6} genomic DNA; no fragment of the *hand2* genomic sequence can be amplified from *han*^{s6} genomic DNA by PCR (Fig. 5B and data not shown), and no portion of *hand2* can hybridize to *han*^{s6} genomic DNA on a Southern blot (data not shown). Furthermore, the deletion of *hand2* segregates with the *han*^{s6} mutant phenotype in 480 meiotic events examined (see Materials and Methods). Analysis of *hand2*-containing PACs indicates that the *han*^{s6} deletion removes less than 100 kb of genomic DNA (see Materials and Methods).

Molecular analysis of the *han*^{c99} mutation provided further evidence that a loss of Hand2 function was responsible for the *han* mutant phenotypes. The coding and untranslated sequences of the *hand2* gene in *han*^{c99} genomic DNA are intact, with the exception of a ~5 kb insertion between bases 346 and 347 of the 5′ untranslated region (UTR) (Fig. 5C,D). This insertion segregates with the *han*^{c99} mutant phenotype in 480 meiotic events examined (see Materials and Methods). We examined the 5′ end of *hand2* mRNA in *han*^{c99} mutants by 5′ RACE and identified insertion-containing messages as well as a splice variant not seen in wild-type embryos. This splice variant eliminates 269 bp of 5′ UTR and 76 bp of coding sequence (Fig. 5C) and could encode a truncated Hand2 protein, with the ATG that normally encodes the forty-sixth residue functioning as the initiation codon.

Altogether, these molecular analyses indicate that *han*^{s6} is a null allele and *han*^{c99} is a hypomorphic allele, consistent with the differences between the *han*^{s6} and *han*^{c99} mutant phenotypes. In an effort to test the hypothesis that a deficiency of *hand2* is sufficient to cause the defects observed in *han*^{s6} mutants, we examined the ability of wild-type *hand2* mRNA to rescue aspects of the *han*^{s6} mutant phenotype. Injecting 100-500 pg of synthetic *hand2* mRNA at the 1- to 4-cell stage can enhance the production of myocardial precursors in a small fraction of injected *han*^{s6} mutant embryos (9 out of 95 injected mutants; Fig. 5E-G). This phenotype appears to represent a partial rescue of *han* function, since we never observed this number of *cmlc2*-expressing myocardial precursors in *han*^{s6} uninjected or *lacZ*-injected siblings (>150 mutant embryos examined).

hand2 expression pattern correlates with locations of *han* function

The early expression of *hand2* in the LPM and the later expression of *hand2* in the heart and pectoral fins correspond well with the timing and location of the defects observed in *han* mutants (Fig. 6). In wild-type zebrafish embryos, *hand2* expression begins at the completion of gastrulation (tailbud stage) in a large portion of the LPM, with its anterior extent just posterior to the head and its posterior extent wrapped around the tailbud (Fig. 6A-C). As convergence and extension proceed, *hand2* expression persists in the LPM (Fig. 6D,E); during somitogenesis, a small gap in *hand2* expression appears (Fig. 6D, arrowheads), producing anterior and posterior expression domains. As the cardiogenic LPM expands, *hand2* transcripts are found in mediolaterally wider domains of the anterior LPM (Fig. 6F), and expression persists in the myocardium as the heart tube forms (Fig. 6K). A mediolateral expansion of *hand2* expression also occurs in the pectoral fin-forming portion of the LPM (Fig. 6G). In this portion of the LPM and in the pectoral fin buds, *hand2*

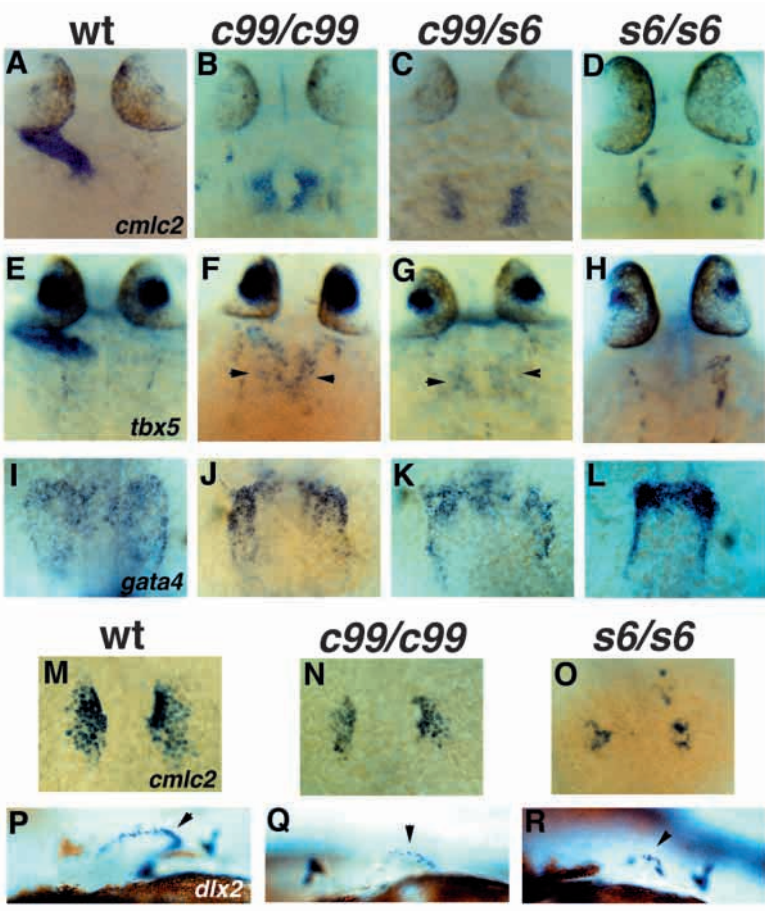

Fig. 4. Comparison of wild-type, *han*^{s6}, *han*^{c99} and *trans*heterozygote phenotypes. (A-O) Dorsal views, anterior to the top. (A,E,I,M,P) Wild-type embryos; (B,F,J,N,Q) *han*^{c99} mutants; (C,G,K) *trans*heterozygous mutants; (D,H,L,O,R) *han*^{s6} mutants. In all cases, the *han*^{s6} phenotype is most severe, the *han*^{c99} phenotype is most mild and the *trans*heterozygote phenotype is intermediate. (A-D) *cmlc2* expression at 24 hpf; (E-H) *tbx5* expression at 24 hpf. Arrowheads (F,G) indicate myocardial tissue. (I-L) *gata4* expression at the 16-somite stage. (M-O) *cmlc2* expression at the 16-somite stage. (P-R) Lateral views of pectoral fin buds, anterior to the left, demonstrating expression of *dlx2* in the apical epidermal fold (arrowheads) at 48 hpf. Continuous and strong *dlx2* expression is observed in the apical fold of wild-type pectoral fins (P) (Akimenko et al., 1994), but *dlx2* maintenance is defective in *han*^{c99} (Q) and *han*^{s6} (R) mutants.

expression appears to overlap with the posterior portion of *tbx5* expression (Fig. 6G-J).

Thus, all of the tissues affected in *han* mutants express *hand2* at the time that defects are apparent. As expected from the molecular analysis of the mutant locus, han^{s6} mutants never express *hand2* at any stage (Fig. 6L and data not shown). han^{c99} mutants exhibit a normal *hand2* expression pattern, although expression levels are significantly and consistently reduced (Fig. 6M and data not shown).

DISCUSSION

The *han* locus encodes Hand2

Our phenotypic and molecular analyses of han^{s6} and han^{c99} mutants provide compelling evidence that the *han* mutant phenotypes are caused by disruption of the *hand2* gene. All of the defects identified in han^{s6} mutants are also present in han^{c99} mutants, although han^{c99} mutants are less severely affected. In agreement with the severity of the phenotypes, the han^{s6} deletion removes the entire *hand2* gene and the han^{c99} insertion alters *hand2* splicing. Furthermore, the expression pattern of *hand2* correlates well with the timing and location of the *han* defects. We therefore conclude that the *han* locus encodes Hand2.

The present data, however, cannot rule out that the han^{s6} and han^{c99} mutations affect other genes besides *hand2*. In particular, there could be a neighboring gene that is removed or influenced by the han^{s6} deletion that is also affected at a distance by the han^{c99} insertion. Without additional *han* alleles available at this time, we favor the simplest interpretation that the han^{s6} and han^{c99} phenotypes reflect the role of Hand2 alone.

Hand2 mediates cardiac differentiation, patterning and morphogenesis

These studies of *han* mutants provide the first evidence that a *hand* gene is required for specific early transitions during myocardial development. Although a normal number of *nkx2.5*-expressing precardiac cells form without Hand2, Hand2 function is essential for their differentiation into *cmlc2*-expressing myocardial precursors. Furthermore, Hand2 is important for generation of *vmhc*-expressing ventricular cells, maintenance of myocardial *tbx5* expression and formation of a midline heart tube. Additionally, Hand2 is critical for an early transition of the cardiogenic LPM, during which the expression domains of LPM genes expand mediolaterally. We hypothesize that this expansion of gene expression reflects the morphogenesis of the LPM through a combination of cell movements and proliferation.

Since *hand2* is expressed broadly within the LPM (in more cells than just the myocardial precursors) and appears to influence the morphogenesis of an extensive portion of the LPM, it seems likely that the role of Hand2 during LPM development begins very early. Even as early as the tailbud stage, Hand2 activity could mediate the LPM response to intrinsic and extrinsic signals that control its subsequent morphogenesis, differentiation and patterning. It is interesting to consider our results from *hand2* mRNA overexpression in light of this model. Overexpression of *hand2* in wild-type embryos does not notably affect the formation of myocardial precursors (D. Y. and D. Y. R. S., unpublished data); however, overexpression of *hand2* in han^{s6} embryos increases the production of myocardial precursors. These data are consistent with Hand2 playing more of a permissive, rather than instructive, role during the selection of myocardial precursors within the LPM. Thus, the lack of efficient or complete rescue of myocardial production in han^{s6} mutants could be due to a requirement for

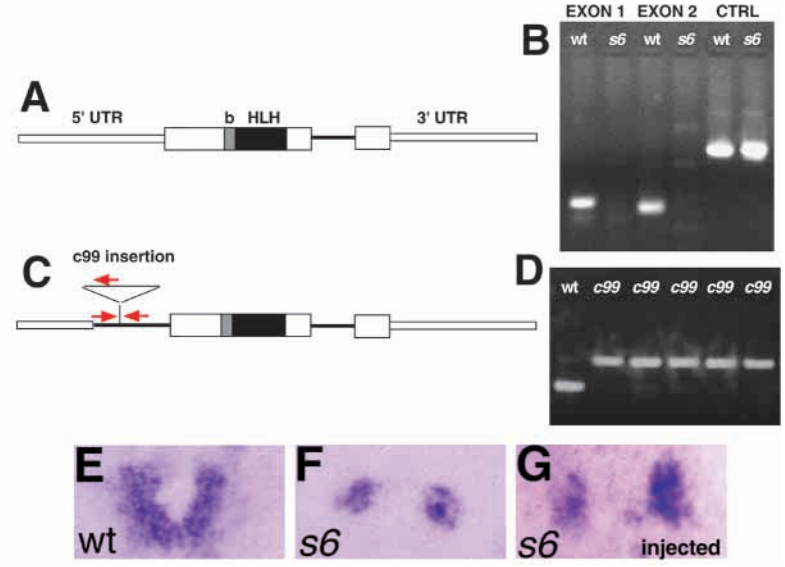

Fig. 5. The *s6* and *c99* mutations disrupt *hand2* genomic DNA. (A) Genomic structure of zebrafish *hand2*. The single intron is represented by a thick horizontal line; 5′ and 3′ UTRs are represented by thin rectangles and the coding regions of the two exons are represented by thick rectangles. A gray rectangle indicates the basic region and a black rectangle indicates the helix-loop-helix domain. (B) No fragment of the *hand2* gene can be amplified by PCR from han^{s6} genomic DNA. Amplifications of a fragment from exon 1, a fragment from exon 2 and a control fragment from the end of a *hand2*-containing PAC are shown; alternating lanes represent reactions performed with wild-type and han^{s6} genomic DNA templates. (C) The han^{c99} mutation is a ~5 kb insertion between bases 346 and 347 of the 5′ UTR. The insertion point is shown with a vertical line; the insertion is not drawn to scale. This insertion can lead to the mis-splicing of *hand2* mRNA at cryptic splice sites at bases 233 and 578. The new 'intron' in this splice variant is represented by a thick line. Some 5′ UTR sequence and some coding sequence are spliced out in this variant. (D) han^{c99} linkage testing was performed using a combination of three PCR primers (shown as red arrows in C, not drawn to scale). When the insertion is absent, the two primers flanking the insertion site amplify a small fragment, as in the case of a homozygous wild-type embryo (first lane). In the presence of the insertion, the flanking primers are ineffective using standard PCR conditions, but the 5′ primer and the primer complementary to the insertion can amplify a slightly larger fragment, as in homozygous han^{c99} mutants (second-sixth lanes). (E-G) Dorsal views of *cmlc2* expression in a wild-type embryo (E), a han^{s6} mutant sibling (F) and a *hand2*-injected han^{s6} mutant sibling (G). All panels are shown at the same magnification. Injection of *hand2* mRNA can partially rescue the production of *cmlc2*-expressing myocardial precursors in han^{s6} mutants. Injection of *hand2* mRNA does not seem to affect the production of myocardial precursors in wild-type embryos (data not shown).

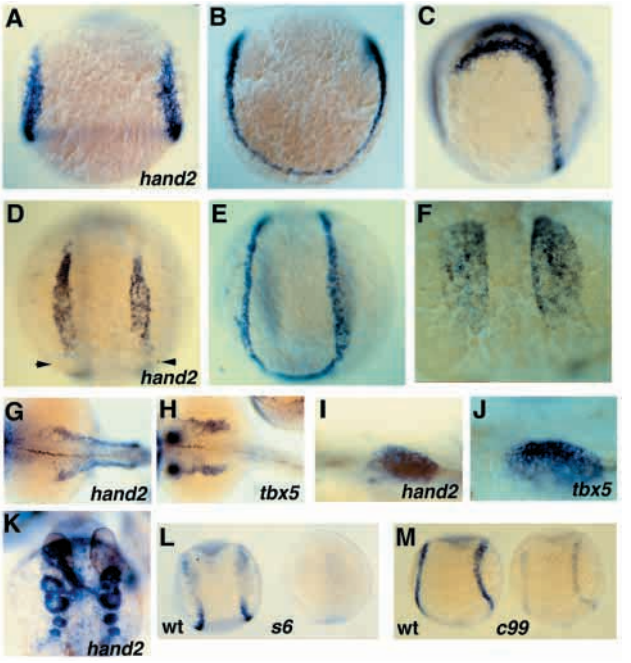

Fig. 6. Expression pattern of zebrafish *hand2*. (A-F) In situ hybridization showing expression of *hand2* in wild-type embryos. (A-C) Three views of the same embryo at tailbud stage (10 hpf), demonstrating *hand2* expression in a continuous streak of the LPM. (A) Dorsal view of anterior part of the embryo, head at the top. (B) Dorsal view of posterior part of the embryo, tailbud at the bottom. (C) Lateral view, anterior to the left. (D,E) Two views of the same embryo at the 10-somite stage, demonstrating *hand2* expression in a large portion of the LPM, with a gap (arrowheads in D) between the anterior and posterior expression domains. (D) Dorsal view of anterior part of the embryo, head at the top. (E) Dorsal view of posterior part of the embryo, tailbud at the bottom. (F) Dorsal view of the cardiogenic portion of the LPM, anterior at the top, demonstrating wider domains of *hand2* expression at the 15-somite stage. (G,H) Dorsal views of the embryonic trunk at the 20-somite stage (19 hpf), anterior to the left, showing gene expression in the bilateral pectoral fin-forming regions of the LPM. *hand2* expression (G) appears to overlap with a posterior portion of *tbx5* expression (H). In H, intense expression of *tbx5* in the dorsal retinae is visible through the yolk at the left side of the image. (I,J) Lateral views, anterior to the left, of pectoral fin buds at 32 hpf. Again, *hand2* expression (I) appears to overlap with a posterior portion of *tbx5* expression (J). (K) Dorsal view through the embryonic head at 28 hpf, anterior to the top. *hand2* is expressed in the midline heart tube as well as within the bilateral sets of branchial arches. *hand2* expression is also faintly visible in a broad sheet of LPM analogous to the *gata4*-expressing tissue shown in Fig. 2F. (L,M) Comparisons of *hand2* expression in *han* mutant and wild-type embryos. Dorsal views, anterior to the top. (L) Wild-type (left) and han^{s6} mutant (right) embryos at the 5-somite stage. Wild-type embryos express *hand2* in the LPM; han^{s6} mutant embryos do not express *hand2* at this or any other stage. (M) *hand2* expression at the 3-somite stage. han^{c99} mutants (right) express lower levels of *hand2* than wild-type siblings (left). *hand2* expression levels are always reduced in han^{c99} mutants, but the locations of *hand2* expression are always normal.

continuous expression of *hand2* within the LPM that cannot be restored by the transient introduction of short-lived mRNA molecules. Complete rescue of han^{s6} mutants may therefore require stable transgenesis using tissue-specific promoters.

Hand2 mediates pectoral fin differentiation, patterning and morphogenesis

Loss of Hand2 function also inhibits pectoral fin outgrowth and differentiation, and Hand2 is essential for *shh* induction in the ZPA. In many respects, the *han* pectoral fin phenotype is similar to that observed in zebrafish *syu* mutants that lack *shh* expression (Neumann et al., 1999; Schauerte et al., 1998). However, there is a clear distinction between the *han* and *syu* phenotypes: Hand2 is essential for an earlier fundamental establishment of AP pattern, as revealed by *hox* gene expression, that is intact in *syu* mutants (Neumann et al., 1999). Additionally, Hand2 function, unlike Shh function (Begemann and Ingham, 2000), is required for the early expansion of the pectoral fin-forming portion of the LPM and for the maintenance of mesenchymal *tbx5* expression from 24 hpf.

The similar themes of the *han* pectoral fin defects and the *han* myocardial defects – early disruption of morphogenesis followed by later defects in differentiation and patterning – reveal parallel roles of Hand2 in heart and forelimb development. Hand2 may promote an analogous state of developmental competence in both the cardiogenic and forelimb-forming portions of the LPM that allows critical morphogenetic transitions, like LPM expansion, to occur. We suspect that these morphogenetic transitions, in turn, would be necessary for proper differentiation. In this regard, it is interesting to note that the influence of Hand2 on pectoral fin development extends beyond the domain of *hand2* expression in the fin-bud mesenchyme. While only a posterior portion of the fin-forming region of the LPM expresses *hand2* (relative to broader *tbx5* expression), reduced Hand2 function affects the morphogenesis of a larger LPM domain and also affects the maintenance of *tbx5* expression throughout the fin bud. This discrepancy suggests that the critical stage for Hand2 function may occur during early somitogenesis, when *hand2* expression extends throughout the fin-forming LPM. Alternatively, Hand2 may play a more specific role in the AP patterning of the fin bud; for example, absence of Hand2 in the posterior of the fin-forming LPM may prevent the localization of posterior determinants from an early stage, and the lack of proper AP coordinates inhibits general morphogenesis and differentiation processes.

The *han* mutant phenotype is more severe than the mouse *hand2* mutant phenotype

Early parallel roles of Hand2 in myocardial development and limb development were not previously revealed by studies of mouse *hand2* mutants (Srivastava et al., 1997). Targeted disruption of the mouse *hand2* gene produces a less severe phenotype than disruption of zebrafish *hand2*. Mouse *hand2* mutants proceed through the early stages of cardiogenesis well, generating a normal number of myocardial precursors that form a midline heart tube. However, at a later stage (E9.5), the right ventricle fails to differentiate, leading to embryonic lethality. No limb phenotypes have previously been reported for the mouse *hand2* mutants.

One possible explanation for this discrepancy is that the bHLH transcription factor gene Hand1, also known as eHAND/Thing-1/Hxt (Cross et al., 1995; Cserjesi et al., 1995; Hollenberg et al., 1995; Srivastava et al., 1995), may compensate for a lack of Hand2 function in mouse *hand2* mutants. Functional redundancy for Hand1 and Hand2 has

been suggested previously by antisense oligonucleotide experiments in chick: oligonucleotides directed against *hand1* and *hand2*, in combination, but not singly, can disrupt cardiac looping (Srivastava et al., 1995). In the mouse embryo, the expression patterns of murine *hand1* and *hand2* overlap significantly, especially within the cardiogenic LPM (Cross et al., 1995; Cserjesi et al., 1995; Biben and Harvey, 1997; Srivastava et al., 1997). Targeted disruption of the mouse *hand1* gene disrupts trophoblast development, making the analysis of cardiac development difficult (Firulli et al., 1998; Riley et al., 1998). However, tetraploid rescue experiments indicate that Hand1 is essential for the morphogenesis and differentiation of the midline heart tube (Riley et al., 1998). Therefore, we speculate that Hand1 and Hand2 can each compensate for the other's absence during early stages of myocardial development in the mouse. Evidently, no such compensation for the loss of *hand2* occurs in zebrafish *han* mutants, and we have not yet detected a zebrafish *hand1*-like gene (Angelo et al., 2000; D. Y. and D. Y. R. S., unpublished data).

Based on the phenotype of mouse *hand2* mutants, previous models of myocardial Hand2 function have suggested that Hand2 regulates chamber-specific differentiation of the right ventricle (Srivastava et al., 1997) or that Hand2 prevents programmed cell death within the right ventricle (Srivastava, 1999; Yamagishi et al., 1999). Our analyses of zebrafish *han* mutants suggest that it is necessary to reevaluate these models, taking into account that Hand proteins appear to play a more general and early role in mediating LPM development, especially LPM morphogenesis and differentiation.

hand2, *tbx5* and a common pathway for heart and forelimb development

In addition to demonstrating a number of specific functions for Hand2 during zebrafish embryogenesis, our studies also highlight the parallels between heart and forelimb development. Several human congenital syndromes include developmental defects in both the heart and limbs (Wilson, 1998); one of these, Holt-Oram syndrome, is caused by mutations in *TBX5* (Basson et al., 1997; Li et al., 1997). Tbx5 has also been shown to regulate cardiac differentiation in *Xenopus* (Horb and Thomsen, 1999) and forelimb differentiation in chick (Gibson-Brown et al., 1998; Isaac et al., 1998; Logan et al., 1998; Ohuchi et al., 1998). The *han* mutant phenotype, especially the poor maintenance of *tbx5* expression in the heart and forelimb, suggests that Hand2, its cofactors and its targets may be relevant to a parallel pathway for heart and forelimb development, as well as to human disorders that occur when this pathway is disrupted.

Other factors are known to play parallel roles in heart and limb development. Fibroblast growth factors (FGFs) have been shown to regulate the induction of cardiac and limb primordia within the LPM. *fgf8* influences *nkx2.5* expression in the zebrafish precardiac mesoderm (Reifers et al., 2000), and a number of different FGFs can induce ectopic limbs in the chick (Martin, 1998). Initial investigations of a mouse mutant that cannot synthesize retinoic acid (RA) (Niederreither et al., 1999), as well as other studies of the functions of RA during embryogenesis (Chazaud et al., 1999; Xavier-Neto et al., 1999; Yelon and Stainier, 1999; Johnson and Tabin, 1997), demonstrate a common role for RA localization in the posteriorization of both the heart and limb. Further examination of Hand2 function is likely to reveal additional similarities between heart and forelimb development and the underlying genetic pathways; it will be especially interesting to examine the relationships between FGFs, RA and Hand2.

We thank C. Miller, X. Sun, G. Martin, A. Schier, A. Joyner, D. Chu and members of the Stainier laboratory for comments on the manuscript, A. Navarro for valuable technical assistance, J. Alexander, A. Rubinstein and M. Macurak for collaboration on genetic screens, M. Ekker, V. Prince, P. Sordino and K. Griffin for plasmids, F. Stockdale for the S46 antibody, and S. Alper for long-range PCR advice. D. Y. was an Amgen fellow of the Life Sciences Research Foundation and is currently the recipient of a Burroughs Wellcome Fund Career Award. M. E. H. acknowledges support from the NIH (DK55390-02). D. Y. R. S. is supported by the NIH, AHA and the David and Lucille Packard Foundation.

Note added in proof

See Charité et al. (*Development* **127**, 2463-2467) for a report of the limb phenotype in mice lacking Hand2. Additional studies of Hand2 function in the limb are reported by Fernandez-Teran et al. (*Development* **127**, 2133-2142).

REFERENCES

Akimenko, M.-A., Ekker, M., Wegner, J., Lin, W. and Westerfield, M. (1994). Combinatorial expression of three zebrafish genes related to *Distal-less*: part of a homeobox gene code for the head. *J. Neurosci.* **14**, 3475-3486.

Alexander, J., Stainier, D. Y. and Yelon, D. (1998). Screening mosaic F1 females for mutations affecting zebrafish heart induction and patterning. *Dev. Genet.* **22**, 288-299.

Amemiya, C. T. and Zon, L. I. (1999). Generation of a zebrafish P1 artificial chromosome library. *Genomics* **58**, 211-213.

Angelo, S., Lohr, J., Lee, K.H., Ticho, B., Breitbart, R., Hill, S., Yost, H.J. and Srivastava, D. (2000). Conservation of sequence and expression of Xenopus and zebrafish dHAND during cardiac, branchial arch, and lateral mesoderm development. *Mech. Dev.* In press.

Bader, D., Masaki, T. and Fischman, D. A. (1982). Immunochemical analysis of myosin heavy chain during avian myogenesis *in vivo* and *in vitro*. *J. Cell Biol.* **95**, 763-770.

Bao, Z. Z., Bruneau, B. G., Seidman, J. G., Seidman, C. E. and Cepko, C. L. (1999). Regulation of chamber-specific gene expression in the developing heart by Irx4. *Science* **283**, 1161-1164.

Basson, C. T., Bachinsky, D. R., Lin, R. C., Levi, T., Elkins, J. A., Soults, J., Grayzel, D., Kroumpouzou, E., Traill, T. A., Leblanc-Straceski, J. et al. (1997). Mutations in human TBX5 cause limb and cardiac malformation in Holt-Oram syndrome. *Nat. Genet.* **15**, 30-35.

Begemann, G. and Ingham, P. W. (2000). Developmental regulation of Tbx5 in zebrafish embryogenesis. *Mech. Dev.* **90**, 299-304.

Biben, C. and Harvey, R. P. (1997). Homeodomain factor Nkx2-5 controls left/right asymmetric expression of bHLH gene eHand during murine heart development. *Genes Dev.* **11**, 1357-1369.

Bruneau, B. G., Bao, Z.-Z., Tanaka, M., Schott, J.-J., Izumo, S., Cepko, C. L., Seidman, J. G. and Seidman, C. E. (2000). Cardiac expression of the ventricle-specific homeobox gene *Irx4* is modulated by Nkx2-5 and dHand. *Dev. Biol.* **217**, 266-277.

Chazaud, C., Chambon, P. and Dollé, P. (1999). Retinoic acid is required in the mouse embryo for left-right asymmetry determination and heart morphogenesis. *Development* **126**, 2589-2596.

Chen, J.-N. and Fishman, M. C. (1996). Zebrafish *tinman* homolog demarcates the heart field and initiates myocardial differentiation. *Development* **122**, 3809-3816.

Chen, J.-N., Haffter, P., Odenthal, J., Vogelsang, E., Brand, M., van Eeden, F. J., Furutani-Seiki, M., Granato, M., Hammerschmidt, M., Heisenberg, C. P. et al. (1996). Mutations affecting the cardiovascular system and other internal organs in zebrafish. *Development* **123**, 293-302.

Cross, J. C., Flannery, M. L., Blanar, M. A., Steingrimsson, E., Jenkins, N. A., Copeland, N. G., Rutter, W. J. and Werb, Z. (1995). Hxt encodes

a basic helix-loop-helix transcription factor that regulates trophoblast cell development. *Development* **121**, 2513-2523.

Cserjesi, P., Brown, D., Lyons, G. E. and Olson, E. N. (1995). Expression of the novel basic helix-loop-helix gene eHAND in neural crest derivatives and extraembryonic membranes during mouse development. *Dev. Biol.* **170**, 664-678.

Firulli, A. B., McFadden, D. G., Lin, Q., Srivastava, D. and Olson, E. N. (1998). Heart and extra-embryonic mesodermal defects in mouse embryos lacking the bHLH transcription factor Hand1. *Nat. Genet.* **18**, 266-270.

Geisler, R., Rauch, G. J., Baier, H., van Bebber, F., Brobeta, L., Dekens, M. P., Finger, K., Fricke, C., Gates, M. A., Geiger, H. et al. (1999). A radiation hybrid map of the zebrafish genome. *Nat. Genet.* **23**, 86-89.

Gibson-Brown, J., Agulnik, S. I., Silver, L. M., Niswander, L. and Papaioannou, V. E. (1998). Involvement of T-box genes Tbx2-Tbx5 in vertebrate limb specification and development. *Development* **125**, 2499-2509.

Goldstein, A. M. and Fishman, M. C. (1998). Notochord regulates cardiac lineage in zebrafish embryos. *Dev. Biol.* **201**, 247-252.

Grandel, H. and Schulte-Merker, S. (1998). The development of the paired fins in the Zebrafish (*Danio rerio*). *Mech. Dev.* **79**, 99-120.

Griffin, K. J. P., Stoller, J., Gibson, M., Chen, S., Yelon, D., Stainier, D. Y. R. and Kimelman, D. (2000). A conserved role for *H15*-related T-box transcription factors in zebrafish and *Drosophila* heart formation. *Dev. Biol.* **218**, 235-247.

Hollenberg, S. M., Sternglanz, R., Cheng, P. F. and Weintraub, H. (1995). Identification of a new family of tissue-specific basic helix-loop-helix proteins with a two-hybrid system. *Mol. Cell. Biol.* **15**, 3813-3822.

Horb, M. E. and Thomsen, G. H. (1999). *Tbx5* is essential for heart development. *Development* **126**, 1739-1751.

Imai, Y., Feldman, B., Schier, A. F., and Talbot, W. S. (2000). Analysis of chromosomal rearrangements induced by postmeiotic mutagenesis with ethylnitrosourea in zebrafish. *Genetics.* In press.

Isaac, A., Rodriguez-Esteban, C., Ryan, A., Altabef, M., Tsukui, T., Patel, K., Tickle, C. and Izpisua-Belmonte, J. C. (1998). Tbx genes and limb identity in chick embryo development. *Development* **125**, 1867-1875.

Johnson, R. L. and Tabin, C. J. (1997). Molecular models for vertebrate limb development. *Cell* **90**, 979-990.

Johnson, S. L., Africa, D., Horne, S. and Postlethwait, J. H. (1995). Half-tetrad analysis in zebrafish: mapping the *ros* mutation and the centromere of linkage group I. *Genetics* **139**, 1727-1735.

Kishimoto, Y., Lee, K. H., Zon, L., Hammerschmidt, M. and Schulte-Merker, S. (1997). The molecular nature of zebrafish *swirl*: BMP2 function is essential during early dorsoventral patterning. *Development* **124**, 4457-4466.

Lee, K. H., Xu, Q. and Breitbart, R. E. (1996). A new tinman-related gene, *nkx2.7*, anticipates the expression of *nkx2.5* and *nkx2.3* in zebrafish heart and pharyngeal endoderm. *Dev. Biol.* **180**, 722-731.

Li, Q. Y., Newbury-Ecob, R. A., Terrett, J. A., Wilson, D. I., Curtis, A. R., Yi, C. H., Gebuhr, T., Bullen, P. J., Robson, S. C., Strachan, T. et al. (1997). Holt-Oram syndrome is caused by mutations in TBX5, a member of the Brachyury (T) gene family. *Nat. Genet.* **15**, 21-29.

Logan, M., Simon, H.-G. and Tabin, C. (1998). Differential regulation of T-box and homeobox transcription factors suggests roles in controlling chick limb-type identity. *Development* **125**, 2825-2835.

Martin, G. R. (1998). The roles of FGFs in the early development of vertebrate limbs. *Genes Dev.* **12**, 1571-1586.

Neumann, C. J., Grandel, H., Gaffield, W., Schulte-Merker, S. and Nüsslein-Volhard, C. (1999). Transient establishment of anteroposterior polarity in the zebrafish pectoral fin bud in the absence of *sonic hedgehog* activity. *Development* **126**, 4817-4826.

Niederreither, K., Subbarayan, V., Dolle, P. and Chambon, P. (1999). Embryonic retinoic acid synthesis is essential for early mouse post-implantation development. *Nat. Genet.* **21**, 444-448.

Ohuchi, H., Takeuchi, J., oshioka, H., Ishimaru, Y., Ogura, K., Takahashi, N., Ogura, T. and Noji, S. (1998). Correlation of wing-leg identity in ectopic FGF-induced chimeric limbs with the differential expression of chick Tbx5 and Tbx4. *Development* **125**, 51-60.

Reifers, F., Walsh, E. C., Léger, S., Stainier, D. Y. R. and Brand, M. (2000). Induction and differentiation of the zebrafish heart requires fibroblast growth factor 8 (*fgf8/acerebellar*). *Development* **127**, 225-235.

Reiter, J. F., Alexander, J., Rodaway, A., Yelon, D., Patient, R., Holder, N. and Stainier, D. Y. R. (1999). Gata5 is required for the development of the heart and endoderm-derived organs in zebrafish. *Genes Dev.* **13**, 2983-2995.

Riley, P., Anson-Cartwright, L. and Cross, J. C. (1998). The Hand1 bHLH transcription factor is essential for placentation and cardiac morphogenesis. *Nat. Genet.* **18**, 271-275.

Ruvinsky, I., Oates, A. C., Silver, L. M. and Ho, R. K. (2000). The evolution of paired appendages in vertebrates: T-box genes in the zebrafish. *Dev. Genes Evol.* **210**, 82-91.

Schauerte, H. E., van Eeden, F. J. M., Fricke, C., Odenthal, J., Strähle, U. and Haffter, P. (1998). Sonic hedgehog is not required for the induction of medial floor plate cells in the zebrafish. *Development* **125**, 2983-2993.

Schultheiss, T. M., Burch, J. B. and Lassar, A. B. (1997). A role for bone morphogenetic proteins in the induction of cardiac myogenesis. *Genes Dev.* **11**, 451-462.

Serbedzija, G. N., Chen, J. N. and Fishman, M. C. (1998). Regulation in the heart field of zebrafish. *Development* **125**, 1095-1101.

Srivastava, D. (1999). HAND proteins: molecular mediators of cardiac development and congenital heart disease. *Trends Cardiovasc. Med.* **9**, 11-18.

Srivastava, D., Cserjesi, P. and Olson, E. N. (1995). A subclass of bHLH proteins required for cardiac morphogenesis. *Science* **270**, 1995-1999.

Srivastava, D., Thomas, T., Lin, Q., Kirby, M. L., Brown, D. and Olson, E. N. (1997). Regulation of cardiac mesodermal and neural crest development by the bHLH transcription factor, dHAND. *Nat. Genet.* **16**, 154-160.

Stainier, D. Y. R. and Fishman, M. C. (1992). Patterning the zebrafish heart tube: acquisition of anteroposterior polarity. *Dev. Biol.* **153**, 91-101.

Stainier, D. Y. R., Fouquet, B., Chen, J. N., Warren, K. S., Weinstein, B. M., Meiler, S. E., Mohideen, M. A., Neuhauss, S. C., Solnica-Krezel, L., Schier, A. F. et al. (1996). Mutations affecting the formation and function of the cardiovascular system in the zebrafish embryo. *Development* **123**, 285-292.

Streisinger, G., Singer, F., Walker, C., Knauber, D. and Dower, N. (1986). Segregation analyses and gene-centromere distances in zebrafish. *Genetics* **112**, 311-319.

Tamura, K., Yonei-Tamura, S. and Izpisúa Belmonte, J. C. (1999). Differential expression of *Tbx4* and *Tbx5* in Zebrafish fin buds. *Mech. Dev.* **87**, 181-184.

Westerfield, M. (1995). The Zebrafish Book. Eugene, OR: Univ. of Oregon Press.

Wilson, G. N. (1998). Correlated heart/limb anomalies in mendelian syndromes provide evidence for a cardiomelic developmental field. *Am. J. Med. Genet.* **76**, 297-305.

Xavier-Neto, J., Neville, C. M., Shapiro, M. D., Houghton, L., Wang, G. F., Nikovits, W. J., Stockdale, F. E. and Rosenthal, N. (1999). A retinoic acid-inducible transgenic marker of sino-atrial development in the mouse heart. *Development* **126**, 2677-2687.

Yamagishi, H., Garg, V., Matsuoka, R., Thomas, T. and Srivastava, D. (1999). A molecular pathway revealing a genetic basis for human cardiac and craniofacial defects. *Science* **283**, 1158-1161.

Yelon, D., Horne, S. A. and Stainier, D. Y. (1999). Restricted expression of cardiac myosin genes reveals regulated aspects of heart tube assembly in zebrafish. *Dev. Biol.* **214**, 23-37.

Yelon, D. and Stainier, D. Y. (1999). Patterning during organogenesis: genetic analysis of cardiac chamber formation. *Semin. Cell Dev. Biol.* **10**, 93-98.